Ion-acoustic supersolitons in plasmas with two-temperature electrons: Boltzmann and kappa distributions

Frank Verheest,[1,2,a)] Manfred A. Hellberg,[2,b)] and Ioannis Kourakis[3,c)]
[1]*Sterrenkundig Observatorium, Universiteit Gent, Krijgslaan 281, B–9000 Gent, Belgium*
[2]*School of Chemistry and Physics, University of KwaZulu-Natal, Durban 4000, South Africa*
[3]*Centre for Plasma Physics, Department of Physics and Astronomy, Queen's University Belfast, BT7 1NN Northern Ireland, United Kingdom*

(Received 4 July 2013; accepted 1 August 2013; published online 21 August 2013)

Acoustic supersolitons arise when a plasma model is able to support three consecutive local extrema of the Sagdeev pseudopotential between the undisturbed conditions and an accessible root. This leads to a characteristic electric field signature, where a simple bipolar shape is enriched by subsidiary maxima. Large-amplitude nonlinear acoustic modes are investigated, using a pseudopotential approach, for plasmas containing two-temperature electrons having Boltzmann or kappa distributions, in the presence of cold fluid ions. The existence domains for positive supersolitons are derived in a methodological way, both for structure velocities and amplitudes, in terms of plasma compositional parameters. In addition, typical pseudopotentials, soliton, and electric field profiles have been given to illustrate that positive supersolitons can be found in the whole range of electron distributions from Maxwellian to a very hard nonthermal spectrum in kappa. However, it is found that the parameter ranges that support supersolitons vary significantly over the wide range of kappa considered. © *2013 AIP Publishing LLC*. [http://dx.doi.org/10.1063/1.4818888]

I. INTRODUCTION

The concept of acoustic supersolitons was introduced by Dubinov and Kolotkov for plasmas with five species,[1,2] but discussed only for a single set of plasma parameters.

Mathematically, supersolitons arise when a plasma model is able to support three consecutive local extrema of the Sagdeev pseudopotential[3] between the undisturbed conditions and an accessible root. This leads to a characteristic supersoliton signature in the electric field, viz., the usual simple bipolar soliton shape is enriched by the presence of a subsidiary maximum on each side of the structure. Electric field structures that are similar in appearance have been observed in space plasmas.[4] Although the authors of Ref. 4 offer an alternative explanation (involving Bernstein-Green-Kruskal modes) for these forms, it is possible that the structures may in fact represent acoustic supersolitons.

Going beyond the initial identification of supersolitons,[1,2] Verheest *et al.*[5,6] have shown that they can also exist in three-component plasmas and established a methodology to define their existence domains in parameter space. Thus, it is clear that these new soliton forms are not an artefact of very special plasmas requiring a larger number of parameters to generate them. Remarkably, many features of supersolitons had been seen in previous papers[7–10] but not recognized as being special.

Ion acoustic solitons in three-species plasmas composed of an ion species and two Boltzmann-distributed electron components having different temperatures have long been a subject of study.[11–18] It is well-known that both positive and negative solitons can be found, and that coexistence occurs, that is, there are regions of parameter space in which either positive or negative potential solitons may occur, depending on initial disturbances. In addition, negative potential double layers were found to act as the limit of the negative soliton existence domain.[15]

Subsequently, Baluku *et al.*[8] found that positive double layers could also exist in such a plasma in a narrow range of parameter space. Although the normalized double layer structure speed, M_{dl}, had in practice often been found to act as the upper limit for soliton existence, Baluku *et al.*[8] showed that solitons could indeed occur beyond that value for these positive potential double layers. It has since turned out that the solitons that arise at speeds beyond M_{dl} are in fact supersolitons. Hence, Ref. 8 showed that plasmas having two Boltzmann-distributed electrons and one fluid ion species can admit positive supersolitons. We note that this form of three-component plasma is in contrast to those considered recently by Verheest *et al.*[5,6] The latter investigations of supersoliton existence domains were carried out in plasmas with only a single component of (Cairns-distributed,[19] nonthermal) electrons, but two inertial species, viz., either two ion species[5] or an ion species, together with massive dust grains.[6]

Although Boltzmann distributions are very often used in the modeling of plasmas, particle velocity distribution functions in space plasmas often exhibit enhanced high-energy (superthermal) tails and are well-fitted by kappa distributions.[20–22] The kappa distribution, a generalization of the Maxwellian, represents a family of velocity distributions, ranging from an extreme "hard" spectrum associated with $\kappa \simeq 1.5 - 2$, to the Maxwell-Boltzmann distribution for $\kappa \to \infty$. Observations in Saturn's magnetosphere[23] have shown that the electron distribution function is best fitted by a double kappa distribution, that is, each of the components of the two-temperature electron distribution is best fitted by its own low-kappa form. Although there is

[a)]Electronic mail: frank.verheest@ugent.be
[b)]Electronic mail: hellberg@ukzn.ac.za
[c)]Electronic mail: i.kourakis@qub.ac.uk

variation in the deduced values of kappa associated with the cool (κ_c) and hot (κ_h) electron components in the inner Kronian magnetosphere,[23] it is noticeable that in general, $\kappa_c < \kappa_h$. Hence, when Baluku and Hellberg[24] studied the effects of low κ on ion-acoustic solitons in a two-electron-temperature plasma, they used $\kappa_c = 2$ and $\kappa_h = 3$ as a representative low-κ case.

However, although the generalization of a Boltzmann distribution to one with highly superthermal electrons yielded solitons and double layers, no positive solitons were found beyond M_{dl} for low-κ distributions.[24] Hence it appeared that, unlike the Boltzmann case,[8] double-kappa electron distributions with low κ do not sustain supersolitons.

Both Refs. 8 and 24 have given a thorough discussion of all possible large amplitude solitons and double layers, but did not specifically address the supersoliton properties. Hence, we propose to return to these models, with a specific focus on parameter regimes which admit supersolitons, for plasmas with cold positive ions and two-temperature superthermal electrons with κ distributions. This includes in the limit $\kappa \to \infty$ the special case where the electrons are Boltzmann-distributed. As in our earlier papers,[5,6,8,24] we will investigate large-amplitude nonlinear acoustic modes, based on a Sagdeev pseudopotential approach,[3] in a frame which is co-moving with the nonlinear wave.

The paper is structured as follows. In Sec. II, we recall the elements of the analytical description, derive the Sagdeev pseudopotential, and address the essential properties, which can guide the numerical discussion in Secs. III–V. Section III is devoted to Boltzmann electrons, for two different but typical values of the electron temperature ratio, and gives the existence ranges in parameter space where supersolitons can be found, amplifying earlier work.[8] Section IV then investigates strongly nonthermal κ distributions, for a case which earlier was not deemed to have positive roots beyond the double layers[24] and hence could not generate supersolitons. We show that even for low κ, supersolitons can in fact exist and elaborate on the reasons for that. Because of some fundamental differences between the Boltzmann and low-κ descriptions, as far as supersolitons are concerned, we address in Sec. V an intermediate case, for moderate κ. Finally, Sec. VI summarizes our findings.

II. BASIC FORMALISM

To explore the occurrence of supersolitons in both κ-distributed plasmas and the limiting case of Boltzmann electrons, we shall consider a three-component model similar to that used by Ref. 24. The cold positive ions and two electron species with different kappa-distributed characteristics of our plasma model are labeled i, c, and h, respectively. The fraction of negative charge residing on the cooler electron species is $f = n_{c0}/n_{i0}$, in terms of the undisturbed densities. The ions are assumed singly charged and cold. Singly charged is not a real restriction, because multiple charges can easily be accommodated by adapting the normalization. Cold ions are a useful simplification, as Baluku and Hellberg[24] have shown that describing the ions as warm and adiabatic only leads to small quantitative changes, and we prefer to concentrate here on essential supersoliton characteristics.

The ions are described by the continuity and momentum equations in normalized variables, referred, amongst others, to a speed $C_a = (T_h/m_i)^{1/2}$, where T_h is the kinetic temperature of the hotter electrons, in the absence of superthermal kappa effects. The space co-ordinate is measured in units of $(\varepsilon_0 T_h/n_{i0}e^2)^{1/2}$. In a frame where the nonlinear structure is stationary ($\partial/\partial t = 0$), all variables tend to their undisturbed values at $x \to -\infty$; and in particular, the electrostatic potential φ (normalized to T_h/e) tends to zero. All densities will be normalized with respect to their equilibrium values.

One can integrate the cold ion equations with respect to x and find that the ion charge density is given by

$$n_i = \frac{1}{\sqrt{1 - \dfrac{2\varphi}{M^2}}}. \tag{1}$$

We note that the ion density contains the normalized speed, $M = V/C_a$, where V is the velocity of the nonlinear structure, seen in an inertial frame. There are thus limitations on φ on the positive side at $\varphi_{\ell i} = M^2/2$, as for larger φ the ion density is no longer defined and in fact reaches infinite compression for $\varphi \to \varphi_{\ell i}$.

As announced in the Introduction, we will adopt kappa distributions for the electrons, in the form[22,24,25]

$$n_c = \left(1 - \frac{\varphi}{\tau[\kappa_c - 3/2]}\right)^{-(\kappa_c - 1/2)}, \tag{2}$$

$$n_h = \left(1 - \frac{\varphi}{\kappa_h - 3/2}\right)^{-(\kappa_h - 1/2)}, \tag{3}$$

where $\tau = T_c/T_h$, and $\kappa_c > 3/2$ and $\kappa_h > 3/2$ are the spectral indices.

The basic set of equations is closed by Poisson's equation

$$\frac{d^2\varphi}{dx^2} + n_i - f n_c - (1-f) n_h = 0, \tag{4}$$

and we have used overall charge neutrality in the undisturbed conditions. After integration, (4) yields an energy-like integral

$$\frac{1}{2}\left(\frac{d\varphi}{dx}\right)^2 + S(\varphi, M) = 0, \tag{5}$$

which can be analyzed as in classical mechanics, in terms of a Sagdeev pseudopotential[3]

$$\begin{aligned} S(\varphi, M) = {} & f\tau\left[1 - \left(1 - \frac{\varphi}{\tau[\kappa_c - 3/2]}\right)^{-(\kappa_c - 3/2)}\right] \\ & + (1-f)\left[1 - \left(1 - \frac{\varphi}{\kappa_h - 3/2}\right)^{-(\kappa_h - 3/2)}\right] \\ & + M^2\left(1 - \sqrt{1 - \frac{2\varphi}{M^2}}\right). \end{aligned} \tag{6}$$

Here, we have explicitly referred to φ and M, because M is to be determined such that solitary structures can exist, whereas the parameters f, τ, κ_c, and κ_h specify the precise composition of the plasma model and can be assumed given. We note that, in the limit $\kappa \to \infty$, the κ-related terms reduce to the usual exponential terms found in Sagdeev potentials for Boltzmann electrons.

We recall that by construction and assumption $S(0,M) = S'(0,M) = 0$, and $S''(0,M) \leq 0$ is required to cause the origin to be a (local) unstable maximum, at least on one side.[26] Derivatives of $S(\varphi,M)$ with respect to φ are denoted by primes. In physical terms, the proper convexity condition, $S''(0,M) \leq 0$, ensures that the nonlinear structures are (super)acoustic in a global sense and this yields the minimal M for their existence

$$M^2 \geq M_s^2 = \left[\frac{f(2\kappa_c - 1)}{\tau(2\kappa_c - 3)} + \frac{(1-f)(2\kappa_h - 1)}{2\kappa_h - 3}\right]^{-1}. \quad (7)$$

Here, M_s, which satisfies $S''(0,M_s) = 0$, is the true normalized acoustic speed in the plasma system. Hence, the ratio M/M_s is the true Mach number in the system, since the reference speed used in the normalization disappears from this ratio. We note that, allowing for differing normalizations, this result agrees with that of Ref. 24 for cold ions.

However, in order to have a solitary wave solution, one needs to encounter a root of $S(\varphi,M)$ outside and accessible from $\varphi = 0$. Single roots give hill- or dip-like solitary waves; whereas for double roots, φ changes from one value at $-\infty$ to another at $+\infty$, typical for double layers (potential kinks).

In the following sections, the existence domains for supersolitons are analyzed in a systematic way, the other types of nonlinear structures having been dealt with in previous papers.[8,24] Furthermore, as shown previously, e.g., in Refs. 8, 24, and 26–30, we also need

$$S'''(0,M_s) = 3\left[\frac{f(2\kappa_c - 1)}{\tau(2\kappa_c - 3)} + \frac{(1-f)(2\kappa_h - 1)}{2\kappa_h - 3}\right]^2 - \frac{f(4\kappa_c^2 - 1)}{\tau^2(2\kappa_c - 3)^2} - \frac{(1-f)(4\kappa_h^2 - 1)}{(2\kappa_h - 3)^2}, \quad (8)$$

because the sign of $S'''(0,M_s)$ determines the sign of the KdV-like solitons.[26,27] By "KdV-like," we mean that such solitons have amplitudes which become arbitrarily small as $M \to M_s$, as do solutions of Korteweg-de Vries (KdV) equations.[27] On the other hand, we call "nonKdV-like" those solitons and double layers whose amplitudes remain finite (nonzero) as $M \to M_s$.[6,8,9,26–29]

To get a feeling for where interesting phenomena might occur, we start the discussion by plotting in Fig. 1 how the critical density fraction, f_c, varies with τ along the curve $S'''(0,M_s) = 0$, for different values of κ_c and κ_h. Analogous figures may be found for the double Boltzmann model in Refs. 8, 12, and 13 and for the double κ case in Ref. 24. Inside these curves, $S'''(0,M_s) < 0$, which yields negative potential KdV-like solitons. On the other hand, outside $S'''(0,M_s) = 0$, KdV-like solitons are positive. From (8), one also notes that there is a κ-dependent critical value τ_c for τ

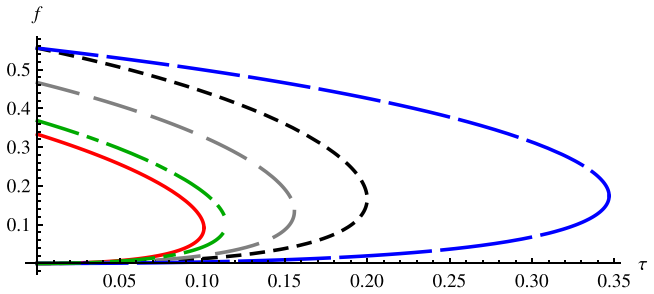

FIG. 1. Variation of the critical charge density fraction, f_c, with τ, along the curve $S'''(0,M_s) = 0$, across which the polarity changes, for Boltzmann ($\kappa_c = \kappa_h = \infty$, solid red curve) and superthermal electrons. Typical κ limits have been plotted, for $\kappa_c = \kappa_h = 3$ (dashed gray curve), $\kappa_c = \kappa_h = 2$ (dotted black curve), $\kappa_c = 2$, $\kappa_h = 3$ (long dashed blue curve), and $\kappa_c = \kappa_h = 10$ (dotted dashed green curve). Inside these curves, $S'''(0,M_s) < 0$ (KdV-like solitons are negative), while outside, $S'''(0,M_s) > 0$ (with positive KdV-like solitons).

beyond which only $S'''(0,M_s) > 0$ is possible, hence no polarity changes can occur and the KdV-like solitons are positive for all f. For $\tau \to 0$, all curves start from $f = 0$ at the lower end and reach an upper end, which depends on κ_c as $(2\kappa_c + 1)/(6\kappa_c - 3)$, and is hence contained between 1/3 (for $\kappa_c = \infty$) and 2/3 (for $\kappa = 3/2$). At the same time, the comparison between the curves for $\kappa_h = 2$ and $\kappa_h = 3$, at the same $\kappa_c = 2$, show that the bulge in τ where the coexistence region ends becomes larger with κ_h. We have tested a whole range of different combinations of κ_c and κ_h and found that indeed τ_c becomes larger as κ_h is increased, at fixed κ_c. Conversely, τ_c is reduced when κ_c is increased, at fixed κ_h. For $\kappa_c = 2$ and $\kappa_h = \infty$, we find that $\tau_c = 0.55$; while for $\kappa_c = \infty$ and $\kappa_h = 2$, that $\tau_c = 0.037$.

Modifications in κ_c and κ_h affect rather significantly the graphs presented in Fig. 1, in a way which is far from being intuitively obvious, and, unfortunately, cannot be pinpointed in analytical expressions. That is why we have refrained from giving, e.g., the explicit solutions for the branches resulting from solving from (8) $S'''(0,M_s) = 0$ for f. These would occupy almost half a page of algebra, contain large and opaque square roots, and yield absolutely no insight.

Supersolitons require pseudopotentials with three local extrema or two distinct wells between $\varphi = 0$ and a negative or a positive root. It follows immediately from (5) that each extremum in $S(\varphi,M)$ must be reflected in a positive or negative extremum in the electric field, thereby generating the characteristic signature of a supersoliton. We briefly recall that, as M is increased, limits on the existence ranges for supersolitons involve first double layers,[5,6,8] which, if they exist, are always lower limits, whereas coalescence of two of the three local extrema, thereby merging the two pseudopotential subwells, can act as lower or upper limits. The transition from double layers to supersolitons is continuous in Mach number M/M_s, but the amplitudes jump in a discontinuous fashion from the double layer to beyond the inaccessible third root of the double layer pseudopotential. Further details are given in Refs. 5 and 6. These limitations can be drawn as curves in $\{f, M/M_s\}$ or in $\{f, \varphi\}$ parameter space, showing the changes as f is increased. All this will be illustrated in more detail below.

First, we note from (6) that $S(\varphi, M) \to -\infty$ (going as $-\sqrt{|\varphi|}$) for $\varphi \to -\infty$. This means that the number of negative roots, if they occur, must be even, given the convexity imposed near $\varphi = 0$. While it is easy enough to find ranges where negative double layers exist, for double Boltzmann electrons[8] or for all admissible κ_c and κ_h,[24] there are no roots with larger amplitudes beyond the negative double layers. The latter possibility would require ultimately four negative roots but the Sagdeev pseudopotential (6) does not contain enough compositional parameters to allow for that. Hence, there can be no negative supersolitons, but only the usual solitons and double layers. As these have been amply investigated in our earlier papers,[8,24] we will omit the discussion of what happens for negative potentials.

On the other hand, previous papers[8,24] have shown that (6) admits positive double layers for double Boltzmann electrons[8] and, indeed, for the whole range of admissible κ_c and κ_h,[24] but only for sufficiently small f and τ. In particular, when considering Boltzmann electrons, no positive double layers have been found for $\tau > \tau_c$ but there are (supersoliton) roots beyond the double layer amplitudes,[8] provided $\tau_{min} < \tau < \tau_c$. Here, τ_{min} denotes the minimum value of τ to allow for the existence of supersolitons. Unfortunately, this has to be determined by numerical trial-and-error; and for lower τ, one might find positive double layers, but then without a third root. This will be discussed further in the different cases we illustrate. As to the case of strong superthermality, at low κ, roots beyond the double layers were not found,[24] which would imply the absence of supersolitons.

However, returning briefly to the discussion of Fig. 1, we see that for given κ_j and fixed τ satisfying $\tau_{min} < \tau < \tau_c$, there are two values for f where the polarity of the KdV-like solitons change, at f_{c1} from positive to negative, and back to positive at f_{c2}. Since there cannot be negative supersolitons, we need in principle to investigate three regimes for possible positive supersolitons: two for $\tau_{min} < \tau < \tau_c$, namely $0 < f < f_{c1}$ and $f > f_{c2}$, and then $0 < f$ for $\tau_c < \tau < \tau_{max}$. Again, increasing τ too far above τ_c might cause the third root of a double layer range to disappear, which signals the end of a supersoliton range. We also add that we have been unable to find positive nonKdV-like double layers, or *a fortiori*, supersolitons.

To illustrate some of the underlying thinking, we show in Fig. 2 three pseudopotentials, having, respectively, three distinct positive roots (red solid curve), a double layer followed by a third root (blue dashed curve), and a single root followed by a double root (green dotted curve). These pseudopotentials have been generated for a specific plasma composition, but at different values of M, which is increasing from top to bottom. The values of f, τ, κ_c, and κ_h are not specified here, as the whole reasoning is generic.

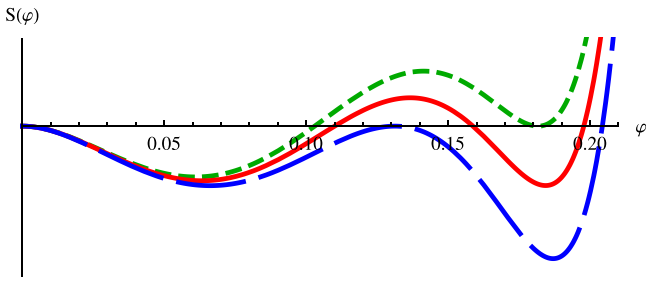

FIG. 2. Example of pseudopotentials having three distinct positive roots (red solid curve), a double layer followed by a third root (blue dashed curve) and a single root followed by a double root (green dotted curve). From top to bottom, the curves correspond to increasing M, for a fixed plasma composition (f, τ, κ_c, and κ_h).

Start with the assumption that there is a pseudopotential with three distinct positive roots, before the infinite ion compression limit at $\varphi_{\ell i}$ comes into play. Here, we note that only the first root is accessible from the undisturbed conditions, and hence this yields a normal soliton. The other roots present no physical interest.

Using now the property that $\partial S/\partial M < 0$ (outside $\varphi = 0$),[30] indicating that at given φ, the value of $S(\varphi, M)$ increases/decreases as M is decreased/increased, we can continuously deform the red solid curve into the green dotted (decrease of M) or the blue dashed curve (increase of M). This means that the first two roots can coalesce for a sufficient increase of M, giving rise to a double layer. A slight further increase yields a supersoliton, because the double layer disappears and the distant third root is now accessible. How long the supersoliton regime lasts as M is increased further, depends on the interplay between the infinite ion compression limit and the merging of the two subwells, the cutoff being governed by whichever occurs at lower M. Since $\varphi_{\ell i}$ increases with the square of M and the double root of the blue dashed curve necessarily lies between the first two roots of the red solid curve, a double layer hence exists for the given plasma composition.

On the other hand, a sufficient decrease of M leads to merging of the last two roots, but that is not physically relevant as both are inaccessible. At the same time, the first accessible root is decreased, giving a soliton of lower amplitude. Further decreases of M reduce the amplitude of the soliton to zero for $M \to M_s$.

As the κ and τ conditions where the third root disappears cannot be established in an analytically meaningful way, we have been forced to determine the appropriate κ values by numerical trial-and-error. As shown in Sec. IV, one can, in fact, find supersolitons at very low κ, but only in ranges other than those that were investigated earlier.[24]

Before studying the characteristics of supersolitons in strongly superthermal plasmas, however, we shall consider in Sec. III the existence of positive supersolitons in plasmas with two Boltzmann species, expanding on previous results.[8] After that we will fast forward to $\kappa_c = 2$ and $\kappa = 3$ in Sec. IV, while we shall provide some remarks and details on intermediate κ values, between 2 and infinity, in Sec. V.

III. BOLTZMANN ELECTRONS ($\kappa_j \to \infty$)

To detect variations in the supersoliton existence domains and amplitudes, we will consider two specific values for τ, namely 0.09, as treated by Baluku *et al.*,[8] and then 0.1, closer to $\tau_c = 0.101$, the critical temperature at which $f_{c1} = f_{c2}$ and beyond which KdV-like solitons are always positive. We hasten to add that we have been unable to find positive double layers either in the second range $f > f_{c2}$ for

$\tau_{min} < \tau < \tau_c$ or in the range where $\tau > \tau_c$, as was already discussed earlier.[8] The minimum value of τ to allow for the existence of supersolitons has been found to be $\tau_{min} = 0.077$. Lower values imply unphysically small f, in effect, a vanishingly small cool electron population.

A. Case $\tau = 0.09$

Given that the presence of two subwells in the Sagdeev pseudopotential is needed to have supersolitons, and that double layers and the creation or destruction of two subwells can introduce other boundaries, we will first delineate existence domains for supersolitons. This is done in Fig. 3 in $\{f, M/M_s\}$ and $\{f, \varphi\}$ parameter space, upper and lower panels, respectively, for $\tau = 0.09$ and $\kappa_c = \kappa_h = \infty$. It turns out from the upper panel of Fig. 3 that the region where positive supersolitons can be found has M values above the green dotted curve (representing the occurrence of positive double layers) or the full red curve (at the emergence of two subwells, for f larger than the value f_{tr} at which the three positive roots coalesce in a triple root), and below the blue dashed curve (merging of two subwells), as M/M_s increases. It is seen that for this value of τ, M is not far above the acoustic speed M_s, and the cool electron fraction (f) is only a few percent.

The lower Fig. 3 has the same coding of the curves, with one essential difference: the introduction of the inaccessible third root of the double layer pseudopotential serves as the minimum amplitude for the supersolitons, indicated by the dark yellow curve with long dashes. We shall adhere to the same styles for the curves in subsequent existence diagrams when τ, κ_c, and κ_h are varied. The amplitudes of the supersolitons lie within the region delimited by this long-dashed curve, the continuous red curve and the blue dashed curve. Comparing the green dotted curve (double layers) and the dark yellow long-dashed curve, we see how big the jump in potential is from the double layer amplitude to the first supersoliton associated with the (now accessible) third root.

Once we know where supersolitons can be found, it is easy to pick appropriate f and M/M_s values and generate plots of pseudopotentials and their associated hodographs. Not wanting to overload the paper, we will restrict ourselves in this subsection to one typical example, as illustrated in Fig. 4. We thus have in the upper panel of Fig. 4 pseudopotentials with a standard soliton (blue dotted curve), a double layer (green dashed curve), and a supersoliton (red solid curve), for $f = 0.01$. There being no negative supersolitons, the negative φ domain has been omitted, here and further below. Our results agree with those of Baluku *et al.*[8] in their Fig. 4. In particular, the double layer velocity $M/M_s = 1.0345$ has been recovered, even though we have used a different normalization. To avoid too much clutter, we did not repeat all the hodographs. However, the big jump in potential to the first supersoliton is again manifested here, following on an increase of only about 0.6% in M/M_s. We also note that in both figures, the existence domains represent a very narrow region, albeit covering a range of values of the two variables considered.

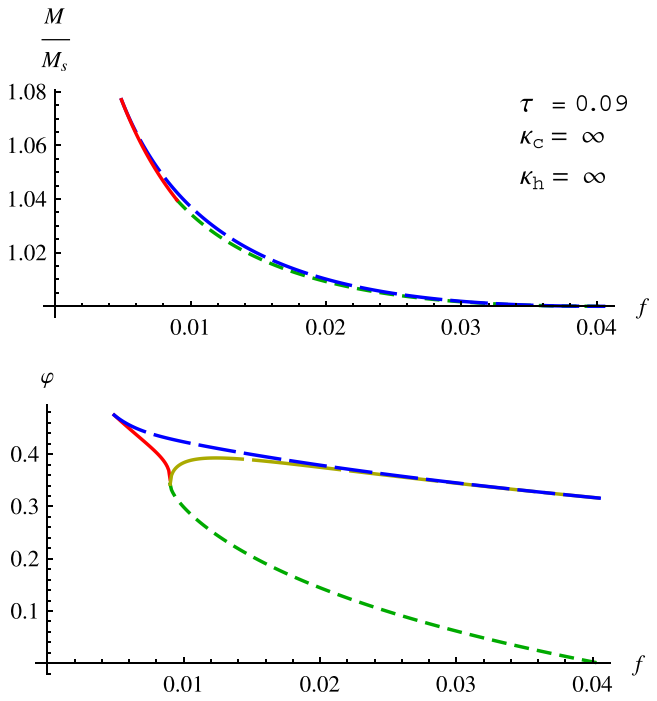

FIG. 3. Upper panel: The region where positive supersolitons can be found is above the green dotted curve (occurrence of negative double layers) or the full red curve (emergence of two subwells), and below the blue dashed curve (merging of two subwells), for $\tau = 0.09$ and $\kappa_c = \kappa_h = \infty$, in the parameter space $\{f, M/M_s\}$. Lower panel: In terms of the amplitudes, the curves have the same coding as in the upper panel, with the addition of the dark yellow long-dashed curve, corresponding to the third root of the double layer pseudopotentials and giving the minimum supersoliton amplitude.

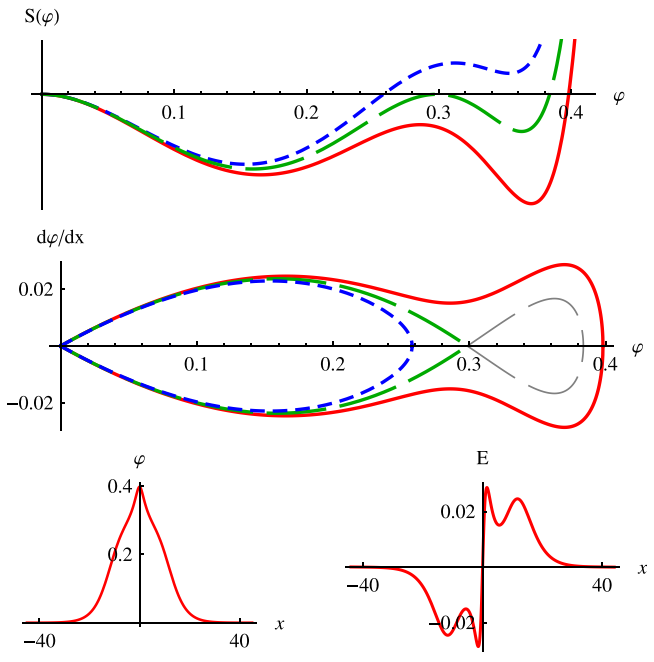

FIG. 4. Upper panel: Pseudopotentials for $f = 0.01$, $\tau = 0.09$, and $\kappa_c = \kappa_h = \infty$, showing a standard soliton (blue dotted curve, $M/M_s = 1.0340$), a double layer (green dashed curve, $M/M_s = 1.0345$), and a supersoliton (red solid curve, $M/M_s = 1.0351$). There being no negative supersolitons, the negative φ domain has been omitted. Middle panel: Hodographs, plotting $d\varphi/dx$ as functions of φ. Thin dashed curves in gray indicate ranges which are not accessible from the undisturbed conditions. Lower panel: Supersoliton potential (left) and electric field (right) profiles, associated with the pseudopotential shown by the red solid curve in the upper panel.

In the middle panel of Fig. 4, the hodographs are presented, plotting $d\varphi/dx$ as functions of φ, with the same curve coding as in the upper panel, and also in similar figures below. Thin dashed curves in gray indicate ranges, which are not accessible from the undisturbed conditions, and this illustrates how the jump in amplitude comes about, from the double layer to the supersoliton amplitude. When the two subwells merge, as M/M_s is increased, the supersoliton range ends, but ordinary solitons are possible for larger M/M_s, until the third root disappears upon encountering the infinite ion compression associated with $\varphi_{\ell i}$.

The lower panel of Fig. 4 then shows the electrostatic potential (left) and electric field (right) profiles of the positive supersoliton associated with the pseudopotential shown by the red solid curve in the upper panel. The small bulges on the potential profile might easily be overlooked, but the wiggles on the electric field are very prominent, and distinguish it from the standard bipolar pulse seen in many space observations.[31,32]

B. Case $\tau = 0.1 < \tau_c = 0.101$

An analogous discussion can be given for smaller or larger τ, but we cannot go beyond $\tau_c = 0.101$, at least, we have been unable to find supersolitons there. We thus pick $\tau = 0.1$ and produce Fig. 5, with similar boundary curves as in Sec. III A. Obvious differences are that the existence ranges are shifted to higher f, but to speeds only marginally above M_s, and reduced amplitudes. Whereas in Fig. 4, it was easy to produce a supersoliton of amplitude around 0.4, it is now difficult to exceed 0.15, as illustrated in Fig. 6 for $f = 0.055$. The supersoliton potential and electric field profiles shown in the lower panel of Fig. 6 are not very different from those in Fig. 4, except that, consistent with the lower speed, the amplitudes are smaller and the widths larger, a

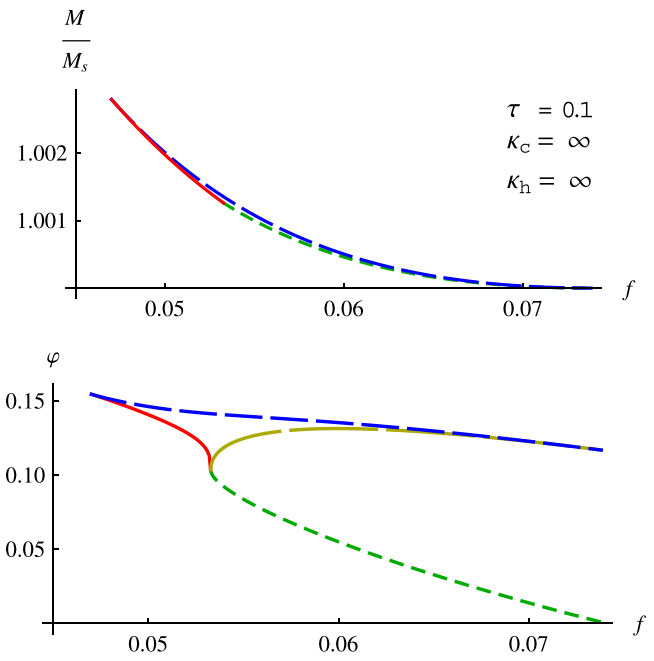

FIG. 5. Existence ranges in the parameter spaces $\{f, M/M_s\}$ (upper panel) and $\{f, \varphi\}$ (lower panel), for $\tau = 0.1$ and $\kappa_c = \kappa_h = \infty$, with the same curve conventions as in Fig. 3.

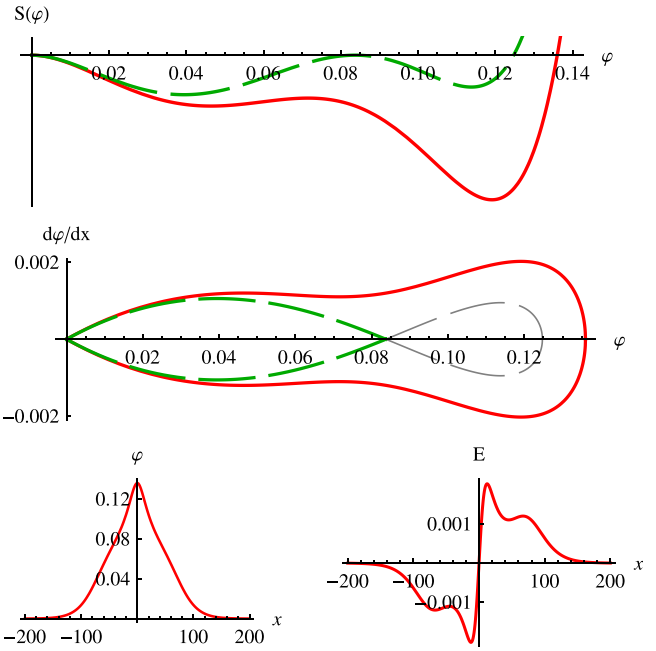

FIG. 6. Upper panel: Pseudopotentials for $f = 0.055$, $\tau = 0.1$, and $\kappa_c = \kappa_h = \infty$, showing a double layer (green dashed curve, $M/M_s = 1.0010$) and a supersoliton (red solid curve, $M/M_s = 1.0011$). Middle and lower panels: As in Fig. 4.

combination of properties that is common to many solitons. However, the bulges on the supersoliton itself are now very slender, so that if one were to peruse only the soliton potential profile, one would be forgiven for regarding it as being normal. The electric field, however, is still very distinctive, but is an order of magnitude smaller than in the previous example.

IV. STRONGLY SUPERTHERMAL ELECTRONS ($\kappa_c = 2$, $\kappa_h = 3$)

We shall now treat a case of strongly superthermal electrons, with $\kappa_c = 2$ and $\kappa_h = 3$, which has not been discussed before in the new light of supersolitons, to the best of our knowledge. This model was investigated by Baluku and Hellberg,[24] but they were unable to identify parameter ranges where a third root would occur beyond the (positive) double layers.

A. Case $\tau = 0.33$

The choice $\tau = 0.33$ obeys not only $\tau < \tau_c = 0.347$, as can be noted from Fig. 1, but also $\tau > \tau_{min} = 0.269$, a minimum value established in an empirical way, at the lower limit of numerical accuracy. Hence, there are two ranges for the positive KdV structures: $0 < f < 0.105$ and $0.255 < f$. Both ranges support positive double layers, but for the lower range, $0 < f < f_{c1} = 0.105$, the double layer pseudopotentials have no other positive roots, as these are cut off due to infinite ion compression at $\varphi_{\ell i}$. Thus, unlike the case of Boltzmann electrons, this lower range of f does not support supersolitons.

In contrast, in the upper range, starting at $f_{c2} = 0.255$, pseudopotentials admit positive double layers plus a root

beyond those, hence supersolitons, but the double layer range ends at $f=0.290$ when all three roots coalesce in a triple root. In the tiny range $0.290 < f < 0.291$, the supersoliton existence is limited between the emergence or disappearance of the two subwells needed to sustain them. The infinite ion compression limit does not come into play for the supersolitons, but it will ultimately limit the existence range of the ordinary solitons which are found beyond the supersoliton range, at increasing M for a given f. It has therefore been omitted from all graphs where the limit due to $\varphi_{\ell i}$ does not play a role in the supersoliton discussion.

Existence diagrams are shown in Fig. 7, which indicate that the range for double layers starts for $f=0.255$ at zero amplitude when $M/M_s = 1$, since we are dealing with KdV-like solitons and double layers. It is interesting that the shape of the existence region differs significantly from that found in Sec. III. This follows because, here, the existence range increases from the critical cool density (here, f_{c2}), at which $S'''(0, M_s)$ changes sign, as M is increased, whereas for the Boltzmann case, the supersoliton range in f decreases from the relevant critical value, f_{c1}, with increasing M.

Pseudopotentials with a positive double layer (dashed green curve) and with a supersoliton (solid red curve) are given in the upper panel of Fig. 8, for $f=0.289$ (close to the upper limit), $\tau = 0.33$, $\kappa_c = 2$ and $\kappa_h = 3$. As in Sec. III, the middle panel of Fig. 8 gives the corresponding hodographs, where again the nonaccessible part of the double layer hodograph has been drawn in light gray.

An important feature to note is that, even though the supersolitons are barely superacoustic, they cannot be described by reductive perturbation theory, even when they are, as here, KdV-like and might have small amplitudes.

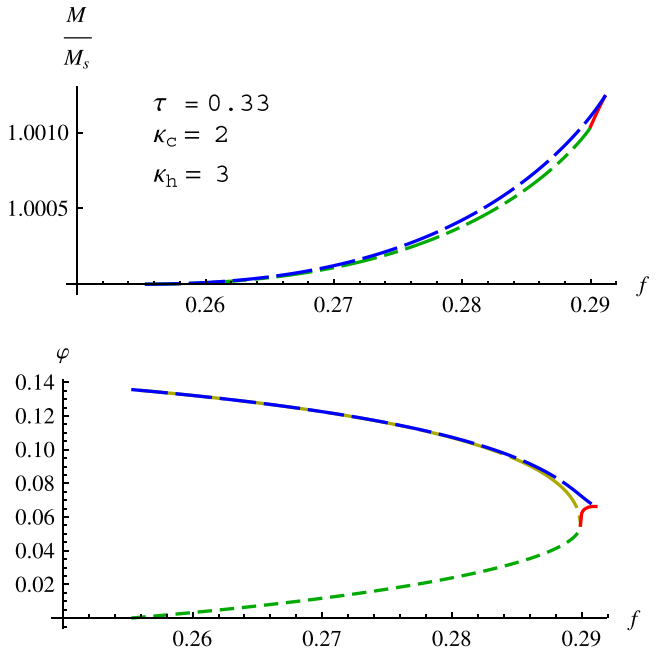

FIG. 7. For $\tau = 0.33$, $\kappa_c = 2$, and $\kappa_h = 3$, the region where positive supersolitons can be found, in terms of M and of φ, with the same curve conventions as in Fig. 3. The double layer range $0 < f < 0.105$ has been omitted for graphical clarity, as it yields no supersolitons.

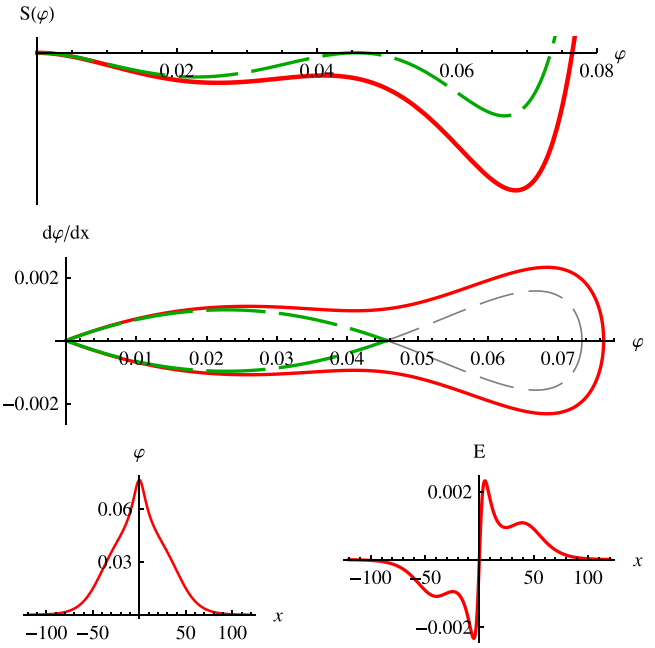

FIG. 8. Upper panel: Pseudopotentials for $f=0.289$, $\tau = 0.33$, $\kappa_c = 2$, and $\kappa_h = 3$, showing a double layer (green dashed curve, $M/M_s = 1.00093$) and a supersoliton (red solid curve, $M/M_s = 1.000097$). Middle and lower panels: As in Fig. 4.

The positive supersoliton potential profile (left) and electric field (right) associated with the pseudopotential shown by the red solid curve in the upper panel of Fig. 8 are shown in the lower panel. When comparing these profiles with those produced in Sec. III for Boltzmann electrons, given in Figs. 4 and 6, we note that the profiles are quite similar, but the associated electric field is weak, an order of magnitude smaller than the example in Sec. III A but of the same order as that in Sec. III B, in line with the very low value of $(M/Ms) - 1$.

At this stage, we want to point out that we have also carried out the corresponding computations for $\tau = 0.34$, at the same κ values. The main difference is a shift to slightly higher f (in the upper range) and higher amplitudes and Mach number. Returning briefly to the perceived lack of third roots beyond the double layer, commented upon in an earlier paper,[24] it appears that, following on the approach used in Ref. 8, only the lower f range was properly investigated. Thus, the supersoliton range discussed here was not found in Ref. 24.

B. Case $\tau = 0.36$

It is clear from Fig. 1 that for $\kappa_c = 2$ and $\kappa_h = 3$, positive KdV-like solitons could occur for $\tau > \tau_c = 0.347$. In searching for supersolitons, we have thus also explored this range, choosing $\tau = 0.36$ as an example. Unlike studies of the Boltzmann case by Ref. 24 and in Sec. III, we have now found both positive double layers and supersolitons. In trying to see whether there might be an upper value, τ_{max}, we have found no limitation, having tested numerically up to unphysically large values such as 0.7, a temperature ratio that is clearly too large to sustain an acceptable distinction between the two electron populations.

The procedure is by now quite standard and starts by finding existence ranges for pseudopotentials with positive double layers and their possible third roots. Since we are no longer in the coexistence domain, we find positive double layers for very low f up to when the triple root is encountered at $f_{tr} = 0.262$. However, the double layer pseudopotentials do not necessarily have a third root. In fact, it only appears from $f = 0.208$ onwards. For lower values of f, the infinite compression limit at $\varphi_{\ell i}$ prevents such roots from occurring. A further associated effect is that the lower limit in soliton speed now exceeds the acoustic speed, unlike the behaviour in the other cases reported above. In addition to the onset of supersolitons beyond a double layer, there is a tiny range $0.262 < f < 0.265$ where the emergence and coalescence of two subwells define the existence range for supersolitons. Together, the range where supersolitons exist is $0.208 < f < 0.265$. This is shown in the existence diagrams in Fig. 9. Starting from the lowest value of f, one finds that the supersolitons are initially (over a very narrow range of f) limited not by the coalescence of the two subwells, but by infinite ion compression. The more usual limit only plays a role when the infinite ion compression occurs at higher values of M/M_s or φ.

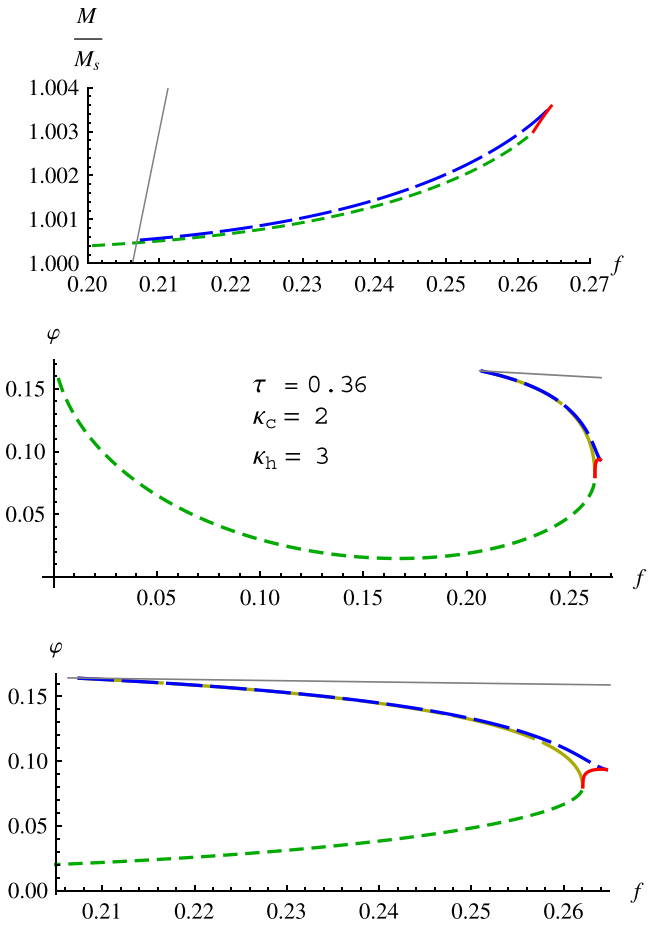

FIG. 9. For $\tau = 0.36$, $\kappa_c = 2$, and $\kappa_h = 3$, the regions are coded as in Fig. 3. In the upper and lower panels, the double layer range has been omitted for $f < 0.2$, in the interest of graphical clarity. It is, however, included in the middle panel to show clearly that double layers exist over a wide range. The thin gray line represents the infinite ion compression limit.

A particular example is illustrated in Fig. 10 for $f = 0.26$, $\tau = 0.36$, $\kappa_c = 2$ and $\kappa_h = 3$, for pseudopotentials with a double layer (green dashed curve) and a supersoliton (red solid curve). As was done before, the middle panel gives the corresponding hodographs. The supersoliton profile (left) and electric field (right) of the positive supersoliton associated with the pseudopotential shown by the red solid curve are shown in the lower panel of Fig. 10. Overall, these figures are similar to those found in Sec. IV A.

V. MODERATELY SUPERTHERMAL ELECTRONS ($\kappa_c = \kappa_h = 10$)

To illustrate how the transition occurs from the Boltzmann picture in Sec. III to the strongly superthermal picture in Sec. IV, we will now investigate appropriate moderate κ values, taking as a typical example, $\kappa_c = \kappa_h = 10$. For such relatively large values of the spectral indices, plasmas are often deemed to be "quasi-Maxwellian." Nonetheless, it turns out that the results differ from those of both Secs. III and IV. As we will show, positive supersolitons can now be found in each of the three possible parameter ranges. From the calculations that underpin the curves in Fig. 1, we infer that $\tau_c = 0.11438$. In addition, it turns out that in this case, there are both lower and upper bounds on τ, with $\tau_{min} = 0.1133$ and $\tau_{max} = 0.1239$. Thus, there is only a narrow range in temperature ratio in which supersolitons can be found.

We would like to add in parentheses that we have thoroughly investigated plasmas with superthermal electrons for the values $\kappa_c = \kappa_h = 2$, 3, and 6. However, such models lead to existence diagrams, pseudopotential examples, and supersoliton potential and electric field profiles which,

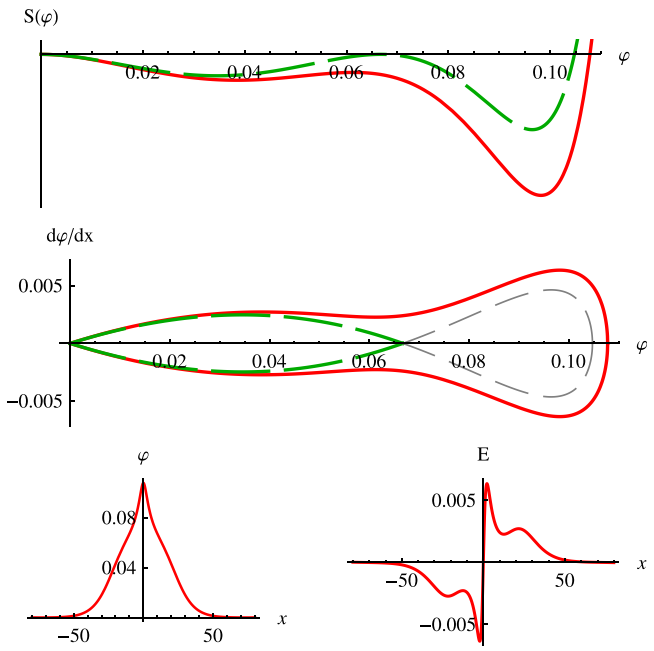

FIG. 10. Upper panel: Pseudopotentials for $f = 0.26$, $\tau = 0.36$, $\kappa_c = 2$, and $\kappa_h = 3$, showing a double layer (green dashed curve, $M/M_s = 1.0027$) and a supersoliton (red solid curve, $M/M_s = 1.0028$). Middle and lower panels: As in Fig. 4.

qualitatively, resemble much of what we have discussed in Sec. IV.

A. Case $\tau = 0.114$

We first consider an example that is just below, but very close to the critical temperature, i.e., $\tau = 0.114 \lesssim 0.11438 = \tau_c$. This is in principle analogous to the double Boltzmann case of Sec. III and Ref. 8. Following the same procedure as in previous sections, we note that $f_{c1} = 0.091$ and $f_{c2} = 0.115$. Unlike for the Boltzmann case, one now finds that in both ranges ($f < f_{c1}$ and $f > f_{c2}$) there are positive double layers and supersolitons, albeit that the upper range turns out to be very limited, $0.115 < f < 0.117$, but it does indeed exist, as shown in Fig. 11.

In the intermediate range, $f_{c1} < f < f_{c2}$, positive solitons can only be nonKdV-like, and they start at the acoustic speed with finite amplitude. Their minimum amplitudes are shown by the dotted yellow curve in part (b) of Fig. 11, a curve computed from the sole positive root of $S(\varphi, M_s)$ in that f range. In fact, this curve in the intermediate range of f connects the two minimum positive supersoliton amplitude limits found in the two adjacent ranges of f. For reasons of analytical continuity, these nonKdV-like positive solitons have minimal amplitudes, which go smoothly over into the amplitude curves of the third positive root when there are positive KdV-like double layers, to the left and right! Otherwise, a small shift in f across the KdV/nonKdV-like boundary would cause an unphysical jump in soliton amplitudes between neighbouring f regions. There are no positive nonKdV-like double layers and hence no supersolitons of that form. On the other hand, in the range $f_{c1} = 0.091 < f < f_{c2} = 0.115$, there are negative double layers that limit the negative KdV-like soliton range, but that is outside the focus of this paper on supersolitons. We note that the overall shape of the existence region is reminiscent of that in Sec. III, but, as discussed above, it is interrupted by the region where the KdV-like solitons reverse polarity. In addition, it is seen that the existence domain is a very narrow strip in parameter space.

A particular example of a supersoliton, illustrative of those found in the lower range ($f < f_{c1}$) is shown in Fig. 12 for $f = 0.01$ and $\tau = 0.114$, for pseudopotentials with a double layer (green dashed curve) and a supersoliton (red solid curve). For graphical clarity, the deep wells of the Sagdeev pseudopotentials have been cut out from Fig. 12. The supersoliton profile (left) and electric field (right) of the positive supersoliton of the pseudopotential shown by the red solid curve in Fig. 12.

The big jump from the double layer amplitude to the smallest supersoliton is again seen not only in part (b) of

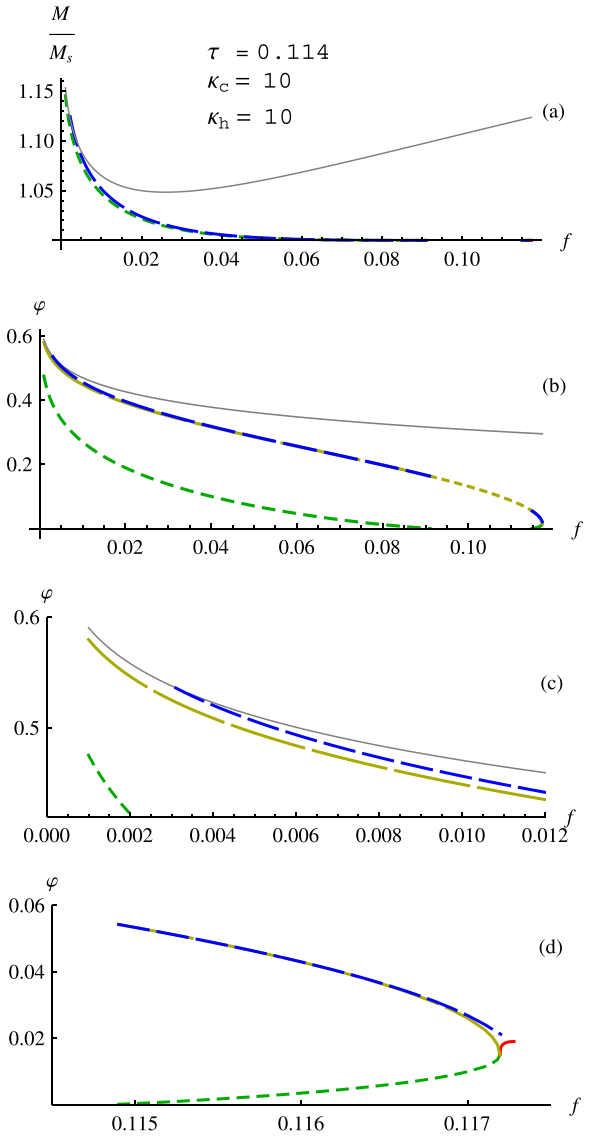

FIG. 11. Existence regions in Mach number and amplitude space, in parts (a) and (b), respectively, for $\tau = 0.114$ and $\kappa_c = \kappa_h = 10$, with the same curve coding as in Fig. 9. A magnification of part (b) is presented in part (c) for the lower and in part (d) for the higher f ranges.

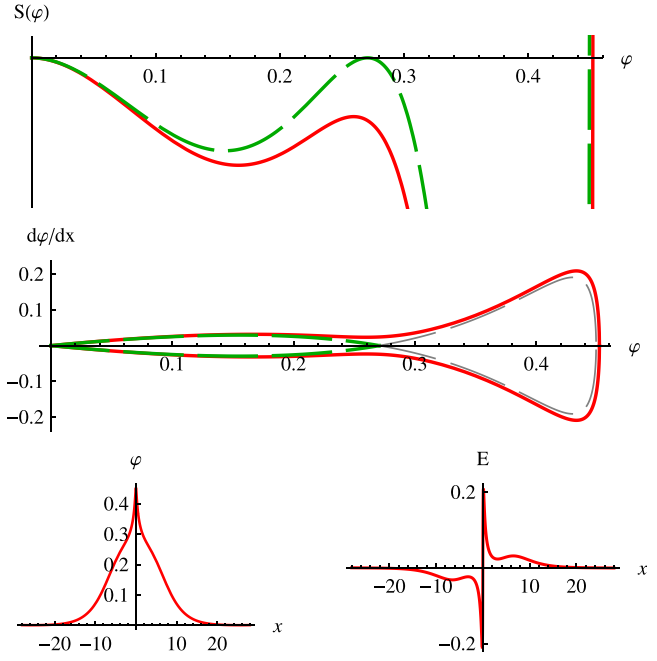

FIG. 12. Upper panel: Pseudopotentials for $f = 0.01$, $\tau = 0.114$, and $\kappa_c = \kappa_h = 10$, showing a double layer (green dashed curve, $M/M_s = 1.0052$) and a supersoliton (red solid curve, $M/M_s = 1.0054$). Middle and lower panels: As in Fig. 4.

Fig. 11, but also on the Sagdeev potential and the hodograph plots in Fig. 12. On the other hand, the deep but narrow second well in the Sagdeev potential curve is reflected in the large bulge on the right of the hodograph and in the large and spiky narrow electric field signature, with only a relatively small wiggle. In addition, it is seen that the potential profile is strongly distorted from the classic soliton shape, because of the strong localized electric field.

We next consider an example of a supersoliton from the upper range of f, namely, $f = 0.117$ and $\tau = 0.114$. This is very close to the upper limit of the supersoliton range in f at this τ. As a result, it is expected from Fig. 11 that both the double layer amplitude and the potential jump to the supersoliton are relatively small (each of order 0.01). This is illustrated in Fig. 13 by pseudopotentials with a double layer (green dashed curve) and a supersoliton (red solid curve). The associated supersoliton potential profile (left) and electric field (right) are shown.

The large hodograph bulge again arises from the deep second Sagdeev pseudopotential well. However, the very weak potential amplitude is now an order of magnitude smaller, and the profile width two orders larger, than in the previous case. As a result, the electric field is much smaller and less spiky, although the relatively deep Sagdeev well of Fig. 13 is still reflected in the distorted soliton shape and the fact that the electric field wiggles are relatively small.

B. Case $\tau = 0.12$

We finally consider a temperature ratio beyond the critical value, namely, $\tau = 0.12$, where we clearly have that $\tau_c < \tau < \tau_{max} = 0.1239$. In this region, all positive solitons are KdV-like, and the double layer range runs from very

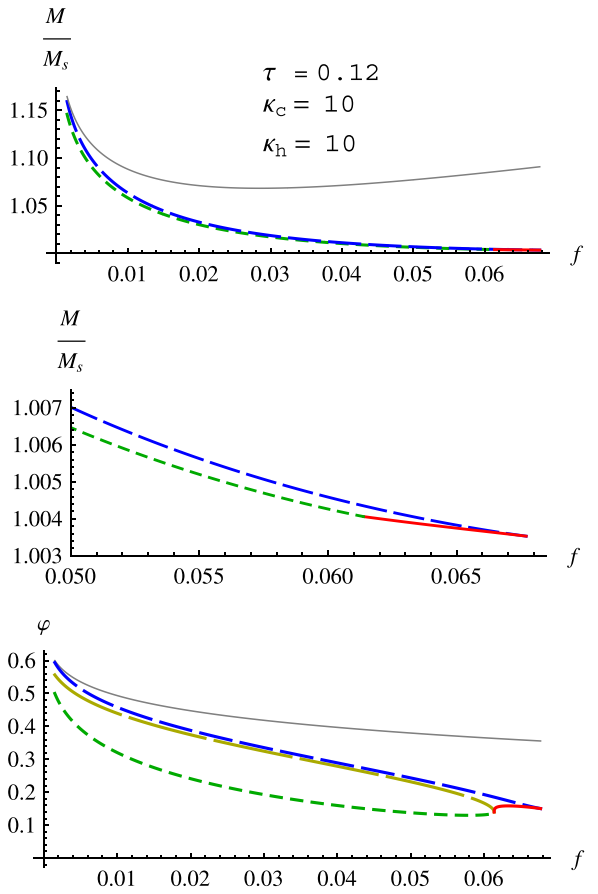

FIG. 14. Existence region in Mach number (upper panel) and amplitude (lower panel) space for $\tau = 0.12$ and $\kappa_c = \kappa_h = 10$, with the same curve coding as in Fig. 9. A magnification of the higher end of the existence curves is presented in the middle panel, for M/M_s.

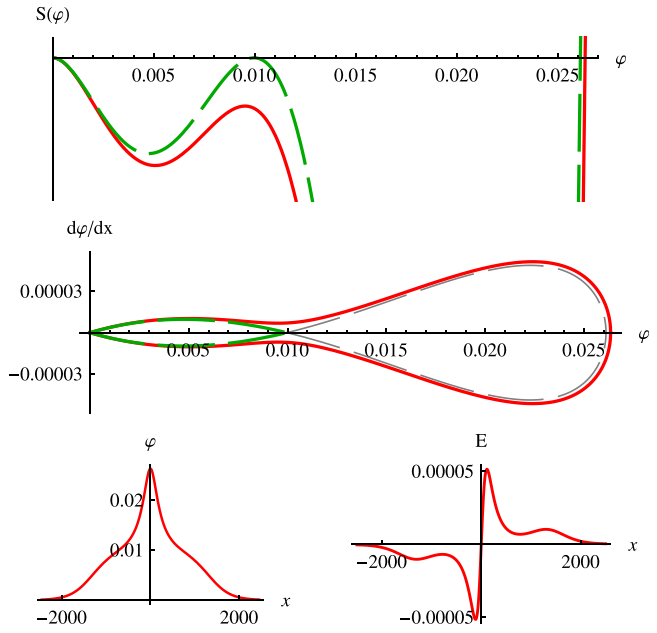

FIG. 13. Upper panel: Pseudopotentials for $f = 0.117$, $\tau = 0.114$, and $\kappa_c = \kappa_h = 10$, showing a double layer (green dashed curve, $M/M_s = 1.0052$) and a supersoliton (red solid curve, $M/M_s = 1.0054$). Middle and lower panels: As in Fig. 4.

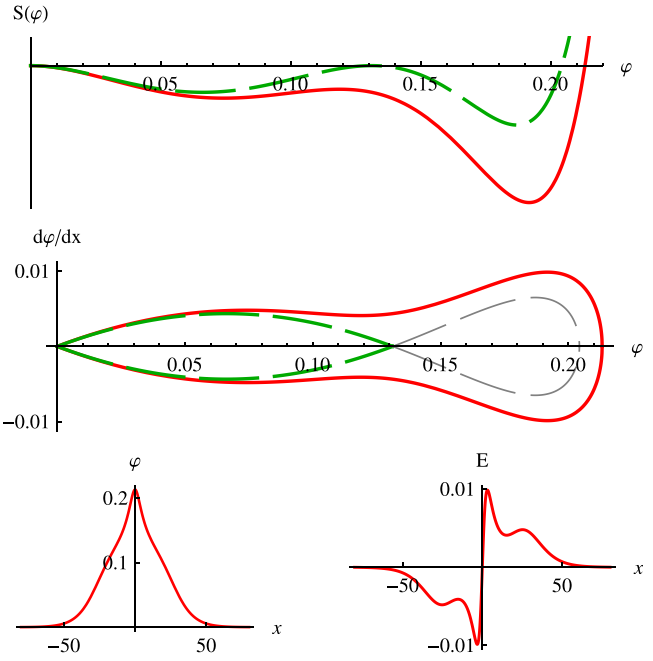

FIG. 15. Upper panel: Pseudopotentials for $f = 0.055$, $\tau = 0.12$, and $\kappa_c = \kappa_h = 10$, showing a double layer (green dashed curve, $M/M_s = 1.0052$) and a supersoliton (red solid curve, $M/M_s = 1.0054$). Middle and lower panels: As in Fig. 4.

small f (for instance, 0.001) up to $f=0.0614$, where a triple root is encountered.

Including the parameter values where the lower limit arises from the forming of a secondary Sagdeev well, the range where supersolitons exist is $0<f<0.0677$. This is shown in the existence diagrams in Fig. 14, which parallel those of Sec. IV B.

A typical supersoliton case is given in Fig. 15 for $f=0.055$, $\tau=0.12$, and $\kappa_c=\kappa_h=10$, for pseudopotentials with a double layer (green dashed curve) and a supersoliton (red solid curve). The lower panel of Fig. 15 gives the corresponding hodographs. The supersoliton profile (left) and electric field (right) of the positive supersoliton associated with the pseudopotential shown by the red solid curve in Fig. 15 are shown. As one might expect, these figures are reminiscent of those found in the region $\tau>\tau_c$ for the strongly nonthermal case of Sec. IV B.

VI. CONCLUSIONS

We have reached the following conclusions:

1. For Maxwellian electrons, the double layer range starts, as f, the relative cool electron density, is increased, from f_{tr}, where pseudopotentials have a positive triple root, and ends at f_{c1} when $M\to M_s$ and the double layer amplitude goes to zero, as long as $\tau_{min}<\tau<\tau_c$, where $\tau=T_c/T_h$. In this whole range $f_{tr}<f<f_{c1}$, the double layer pseudopotentials have a third (inaccessible) root, which serves as the minimum amplitude for supersolitons. There is, in addition, a limited range $f<f_{tr}$ where supersolitons occur, between emergence and merging of two distinct subwells, a range initiated at the merger of all three local extrema. In the ranges $f>f_{c2}$ (for $\tau_{min}<\tau<\tau_c$) and $\tau>\tau_c$, there are no positive double layers nor supersolitons.
2. At the opposite end of the scale, where the two-temperature electrons present a hard spectrum for low κ, as is typical of, for instance, Saturn's magnetosphere, there are two ranges in f for $\tau_{min}<\tau<\tau_c$ where double layers are found: $0<f<f_{c1}$ and $f_{c2}<f<f_{tr}$. In the lower range, the infinite ion compression limit prevents a third root from occurring, hence there can be no supersolitons. However, the double layer pseudopotentials do have a third root in the upper f range, and hence supersolitons can exist, up to where the three local extrema coalesce, just beyond f_{tr}. We note that for this low-kappa case, the triple root occurs at the end of the upper f range, whereas for Boltzmann electrons, it initiated the double layer range for low f. Moreover, when $\tau>\tau_c$, there are now double layers in the range $0<f<f_{tr}$. Supersolitons occur in the higher part of this range, when the ion compression no longer prevents a third root from occurring. This result contradicts an earlier report by Ref. 24 who did not find any supersolitons for this plasma model. It appears that they explored only the Boltzmann-like lower range in f for $\tau<\tau_c$, discussed above. Furthermore, supersolitons are also found in κ-distributed plasmas for $\tau_c<\tau<\tau_{max}$. For the Saturnian case, no obvious physically realistic value of τ_{max} was found, but τ_{max} decreases as the κ_j are increased, and for the intermediate case ($\kappa_j=10$), the range in τ is very narrow.
3. The transition between the two extreme cases of Boltzmann and hard spectrum electron populations occurs around $\kappa_c=\kappa_h=10$, when there are double layers on both f ranges for $\tau_{min}<\tau<\tau_c$, and the triple root is shifted from the lower to the upper range. This starts with a minute upper double layer range, for $\tau_{min}<\tau<\tau_c$ but τ very close to τ_c. This also signals the existence of supersolitons in both ranges, although initially the supersoliton range for $f_{c2}<f<f_{tr}$ is mostly symbolic, with very small amplitudes, and M barely above M_s, and their determination is at the limit of numerical accuracy and physical acceptability. As κ_c and κ_h are further decreased, the range for $0<f<f_{c1}$ retains the double layer existence, but loses the possibility of having a third root, i.e., allowing supersolitons to exist.
4. What seems to be the case is that for Boltzmann and high-κ electrons (the latter usually considered as quasi-Maxwellian), one finds that the triple root at f_{tr} initiates the double layer range in the lower f range, for $\tau_{min}<\tau<\tau_c$. There are no other double layer ranges. When increasing the superthermal content of the distribution (decreasing κ), as soon as the triple root shifts from the lower to the upper range and ends the double layer range, one can have double layers with a third root for all three f ranges. Further decreases of κ kill the third root of the lower range ($0<f<f_{c1}$), but the upper range ($f_{c2}<f<f_{tr}$) retains it, for $\tau_{min}<\tau<\tau_c$. This is also the case for the higher part of the range $f<f_{tr}$, when $\tau_c<\tau<\tau_{max}$. Unfortunately, the precise values of τ_{min} and τ_{max} depend in a nontrivial way on κ_c and κ_h, and have therefore to be determined in a numerical trial-and-error fashion, which provides no physical insight. For very low kappa, there does not seem to be a physically acceptable τ_{max}.
5. It is common in space observations to find plasmas with two-temperature electrons,[33,34] and to find kappa distributions.[35] In the earlier work of Ref. 24, no supersolitons were found for a strongly nonthermal two-temperature plasma typical of Saturn's magnetosphere.[23] It thus left open the question of how common supersolitons may be in space environments, other than those with a double Boltzmann distribution. However, our findings now show that supersolitons should be observable in two-electron-temperature space plasmas over the complete range of kappa values from Boltzmann to a very hard spectrum, albeit for low cool electron fractions, narrow ranges in (f,M) space and, in some cases, in temperature ratio, τ.
6. The model discussed in this paper can be converted, with the appropriate changes in normalizations and polarities, to describe, e.g., dust-acoustic supersolitons in a plasma with cold negative dust and two-temperature Boltzmann or κ-distributed ions, when almost all electrons have been accreted onto the dust. Compared to our earlier supersoliton papers,[5,6] the present model has a quite different composition, but together they illustrate that one can find supersolitons in widely varying three-component plasmas.

Finally, we reiterate the fact that, although in some instances one finds supersolitons that have small normalized amplitudes and are only barely super-acoustic (with M/M_s only marginally above 1), the supersoliton phenomenon cannot be recovered from a KdV approach.

ACKNOWLEDGMENTS

M.A.H. thanks the National Research Foundation of South Africa for partial support under Grant No. 68911. He acknowledges that opinions, findings, and conclusions or recommendations expressed in any publication generated by NRF-supported research are those of the authors, and that the NRF accepts no liability whatsoever in this regard. I.K. warmly acknowledges support from the UK Engineering and Physical Sciences Research Council (EPSRC) via Grant No. EP/I031766/1.

[1]A. E. Dubinov and D. Yu. Kolotkov, IEEE Trans. Plasma Sci. **40**, 1429 (2012).
[2]A. E. Dubinov and D. Yu. Kolotkov, High Energy Chem. **46**, 349 (2012).
[3]R. Z. Sagdeev, *Reviews of Plasma Physics*, edited by M. A. Leontovich (Consultants Bureau, New York, 1966), Vol. 4, p. 23.
[4]J. S. Pickett, L.-J. Chen, S. W. Kahler, O. Santolík, D. A. Gurnett, B. T. Tsurutani, and A. Balogh, Ann. Geophys. **22**, 2515 (2004).
[5]F. Verheest, M. A. Hellberg, and I. Kourakis, Phys. Plasmas **20**, 012302 (2013).
[6]F. Verheest, M. A. Hellberg, and I. Kourakis, Phys. Rev. E **87**, 043107 (2013).
[7]F. Verheest, Phys. Plasmas **16**, 013704 (2009).
[8]T. K. Baluku, M. A. Hellberg, and F. Verheest, Europhys. Lett. **91**, 15001 (2010).
[9]F. Verheest, Phys. Plasmas **18**, 083701 (2011).
[10]A. Das, A. Bandyopadhyay, and K. P. Das, J. Plasma Phys. **78**, 149 (2012).
[11]B. Buti, Phys. Lett. A **76**, 251 (1980).
[12]K. Nishihara and M. Tajiri, J. Phys. Soc. Jpn. **50**, 4047 (1981).
[13]M. Tajiri and K. Nishihara, J. Phys. Soc. Jpn. **54**, 572 (1985).
[14]S. Baboolal, R. Bharuthram, and M. A. Hellberg, J. Plasma Phys. **41**, 341 (1989).
[15]S. Baboolal, R. Bharuthram, and M. A. Hellberg, J. Plasma Phys. **44**, 1–23 (1990).
[16]S. S. Ghosh, K. K. Ghosh, and A. N. Sekar Iyengar, Phys. Plasmas **3**, 3939 (1996).
[17]S. S. Ghosh and A. N. Sekar Iyengar, Phys. Plasmas **4**, 3204 (1997).
[18]J. F. McKenzie, T. B. Doyle, M. A. Hellberg, and F. Verheest, J. Plasma Phys. **71**, 163 (2005).
[19]R. A. Cairns, A. A. Mamun, R. Bingham, R. Boström, R. O. Dendy, C. M. C. Nairn, and P. K. Shukla, Geophys. Res. Lett. **22**, 2709, doi:10.1029/95GL02781 (1995).
[20]V. M. Vasyliunas, J. Geophys. Res. **73**, 2839, doi:10.1029/JA073i009p02839 (1968).
[21]D. Summers and R. M. Thorne, Phys. Fluids B **3**, 1835 (1991).
[22]M. A. Hellberg, R. L. Mace, T. K. Baluku, I. Kourakis, and N. S. Saini, Phys. Plasmas **16**, 094701 (2009).
[23]P. Schippers, M. Blanc, N. André, I. Dandouras, G. R. Lewis, L. K. Gilbert, A. M. Persoon, N. Krupp, D. A. Gurnett, A. J. Coates, S. M. Krimigis, D. T. Young, and M. K. Dougherty, J. Geophys. Res. **113**, A07208, doi:10.1029/2008JA013098 (2008).
[24]T. K. Baluku and M. A. Hellberg, Phys. Plasmas **19**, 012106 (2012).
[25]T. K. Baluku and M. A. Hellberg, Phys. Plasmas **15**, 123705 (2008).
[26]F. Verheest, M. A. Hellberg, and T. K. Baluku, Phys. Plasmas **19**, 032305 (2012).
[27]T. K. Baluku, M. A. Hellberg, I. Kourakis, and N. S. Saini, Phys. Plasmas **17**, 053702 (2010).
[28]T. K. Baluku and M. A. Hellberg, Plasma Phys. Controlled Fusion **53**, 095007 (2011).
[29]F. Verheest and M. A. Hellberg, Phys. Plasmas **17**, 102312 (2010).
[30]F. Verheest, Phys. Plasmas **17**, 062302 (2010).
[31]R. E. Ergun, C. W. Carlson, J. P. McFadden, F. S. Mozer, L. Muschietti, I. Roth, and R. J. Strangeway, Phys. Rev. Lett. **81**, 826 (1998).
[32]D. L. Newman, M. V. Goldman, and R. E. Ergun, Phys. Plasmas **9**, 2337 (2002).
[33]W. C. Feldman, J. R. Ashbridge, S. J. Bame, M. D. Montgomery, and S. P. Gary, J. Geophys. Res. **80**, 4181, doi:10.1029/JA080i031p04181 (1975).
[34]S. Perraut, H. de Feraudy, A. Roux, P. M. E. Décréau, J. Paris, and L. Matson, J. Geophys. Res. **95**, 5997, doi:10.1029/JA095iA05p05997 (1990).
[35]V. Pierrard and M. Lazar, Sol. Phys. **267**, 153 (2010).